Establishment of NOD-*Pdcd1*$^{-/-}$ mice as an efficient animal model of type I diabetes

Jian Wang*†‡, Taku Yoshida‡§¶, Fumio Nakaki*, Hiroshi Hiai‖, Taku Okazaki*†, and Tasuku Honjo§**

Departments of *Medical Chemistry and Molecular Biology and §Immunology and Genomic Medicine and †21st Century Center of Excellence Program, Graduate School of Medicine, and ¶Department of Immunology and Cell Biology, Graduate School of Biostudies, Kyoto University, Yoshida-Konoe, Sakyo-ku, Kyoto 606-8501, Japan; and ‖Shiga Medical Center Research Institute, Moriyama, Shiga 524-8524, Japan

Contributed by Tasuku Honjo, July 4, 2005

Mice deficient in programmed cell death 1 (PD-1, *Pdcd1*), an immunoinhibitory receptor belonging to the CD28/cytotoxic T lymphocyte-associated antigen-4 family, spontaneously develop lupus-like autoimmune disease and autoimmune dilated cardiomyopathy on C57BL/6 and BALB/c backgrounds, respectively. However, how PD-1 deficiency induces different forms of autoimmune diseases on these two strains was unknown. Here, we report that PD-1 deficiency specifically accelerates the onset and frequency of type I diabetes in NOD (nonobese diabetic) mice, with strong T helper 1 polarization of T cells infiltrating into islets. These results suggest that PD-1 deficiency accelerates autoimmune predisposition of the background strain, leading to the induction of different forms of autoimmune diseases depending on the genetic background of the strain. Using NOD-*Pdcd1*$^{-/-}$ mice as an efficient animal model of type I diabetes, we screened diabetes-susceptible loci by genetic linkage analysis. The diabetic incidence of NOD-*Pdcd1*$^{-/-}$ mice was controlled by five genetic loci, including three known recessive loci [*Idd* (insulin-dependent diabetes) *1*, *Idd17*, and *Idd20*] and two previously unidentified dominant loci [*Iddp* (*Idd* under PD-1 deficiency) *1* and *Iddp2*].

autoimmunity | coreceptor | *Idd* locus | Th1 | linkage analysis

Multiple genes are involved in the initiation and progression steps of the organ-specific autoimmune diseases. In theory, these genes could be classified into two groups: (*i*) genes involved in general immune responses, such as cytokines, and (*ii*) genes involved in the organ specificity, such as MHC. Extensive genetic linkage studies have been carried out on human families as well as animal models of various autoimmune diseases to identify responsible genetic loci for autoimmune diseases (1–3). The NOD (nonobese diabetic) mouse, an animal model of type I diabetes, greatly contributed to the understanding of the genetic basis of type I diabetes (4–6). So far, 28 susceptible loci [*Idd* (insulin-dependent diabetes) *1-3*, *4.1*, *4.2*, *5.1*, *5.2*, *6-8*, *9.1*, *9.2*, *9.3*, and *10-24*) have been identified on the NOD chromosomes by several different crosses and generation of congenic mice.

Although many diabetes-susceptible loci have been identified by using NOD mice, the identification of their responsible genes and/or the analyses of the immunological function of each locus have not been carried out smoothly. The difficulty is likely due in part to the late onset and the low penetrance of type I diabetes in NOD mice (40–70% and 20–40% at 30 weeks of age for females and males, respectively) and also to the involvement of many genes. Therefore, the establishment of a better animal model of type I diabetes is required for efficient and refined genetic analyses of type I diabetes. In addition, the low penetrance of the disease in the NOD mouse made the linkage analyses possible only with BC1 (backcross 1) progenies by backcrossing F1 mice on NOD mice, by which dominant loci could not be analyzed (7).

Programmed cell death 1 (PD-1, *Pdcd1*), an immunoreceptor belonging to the CD28/cytotoxic T lymphocyte-associated antigen-4 family, provides negative costimulation by recruiting a protein tyrosine phosphatase, SHP-2 (src homology 2 domain-containing tyrosine phosphatase 2), upon interaction with its ligands, PD-L1 and PD-L2 (8–10). Negative costimulation is required to suppress inappropriate immune responses such as autoimmunity and sustained inflammation. PD-1 knockout mice (*Pdcd1*$^{-/-}$ mice) develop various autoimmune diseases depending on the genetic background. C57BL/6-*Pdcd1*$^{-/-}$ mice develop lupus-like glomerulonephritis and arthritis (11); BALB/c-*Pdcd1*$^{-/-}$ mice produce anti-cardiac troponin I autoantibodies, which are responsible for dilated cardiomyopathy (12, 13). The development of different kinds of autoimmune disease on different genetic backgrounds by PD-1 deficiency lead us to assume that PD-1 deficiency may exaggerate the genetic predisposition of autoimmune diseases such as diabetes in NOD mice.

Here, we report that NOD-*Pdcd1*$^{-/-}$ mice developed type I diabetes by 11 weeks with complete penetrance. Genetic linkage analyses on BC1 backcross progenies of NOD-*Pdcd1*$^{-/-}$ mice revealed that only 3 loci showed significant association with the diabetic incidence among the 28 *Idd* loci described previously using original NOD mice. Using NOD-*Pdcd1*$^{-/-}$ mice, we found that ≈20% of F2 intercross progenies developed diabetes by 15 weeks of age, allowing us to identify two previously unrecognized dominant susceptible loci, *Iddp* (*Idd* under PD-1 deficiency) *1* and *Iddp2*.

Materials and Methods

Animals. NOD/Shi.Jic mice were purchased from Japan Clea (Hamamatsu, Japan). NOD-*Pdcd1*$^{-/-}$ mice were generated by backcrossing C57BL/6-*Pdcd1*$^{-/-}$ mice (11) on NOD WT mice five to eight times. All experiments except for the diabetes incidence experiment (Fig. 1 *a* and *b*) were done with eighth-generation mice. F2 progenies were generated by crossing (NOD-*Pdcd1*$^{+/-}$ × C57BL/6-*Pdcd1*$^{-/-}$)F1 mice with F1 mice. BC1 progenies were generated by crossing (NOD-*Pdcd1*$^{+/-}$ × C57BL/6-*Pdcd1*$^{-/-}$)F1 mice with NOD-*Pdcd1*$^{+/-}$ mice. *Pdcd1*$^{-/-}$ mice were chosen for subsequent analyses. All animals were maintained under specific pathogen-free conditions at the Institute of Laboratory Animals at the Graduate School of Medicine, Kyoto University, and all mouse protocols were approved by the Institute of Laboratory Animals.

Histological Analysis. Insulitis was scored according to the published criteria (14). Briefly, grade 1 represents periinsulitis with mononuclear cell infiltration in <20% of the area of each islet, grade 2 represents moderate insulitis with mononuclear cell infiltration in 20–50% of the area of each islet, and grade 3 represents severe insulitis with mononuclear cell infiltration in >50% of the area of each islet. Sialoadenitis was scored accord-

Abbreviations: PD-1, programmed cell death 1; NOD, nonobese diabetic; *Idd*, insulin-dependent diabetes; *Iddp*, *Idd* under PD-1 deficiency; BC1, backcross 1; lod, logarithm of odds; Th, T helper; DC, dendritic cell.

‡J.W. and T.Y. contributed equally to this work.

**To whom correspondence should be addressed. E-mail: honjo@mfour.med.kyoto-u.ac.jp.

IMMUNOLOGY

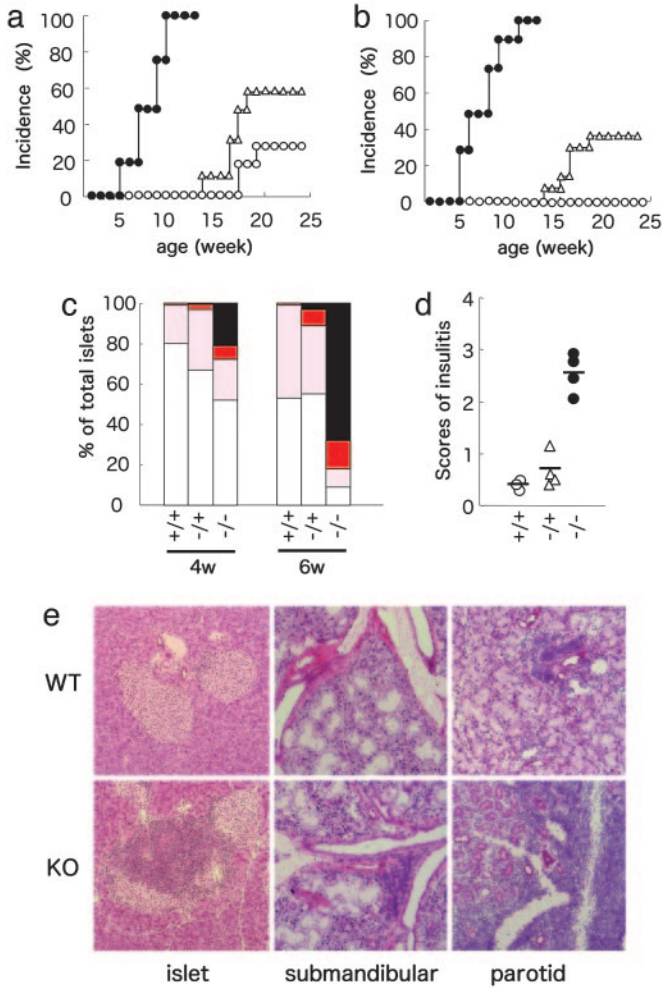

Fig. 1. The early onset and complete penetrance of type I diabetes in NOD-*Pdcd1*$^{-/-}$ mice. (*a*) Incidence of type I diabetes in female NOD-*Pdcd1*$^{-/-}$ (filled circles), NOD-*Pdcd1*$^{+/-}$ (triangles), and NOD WT (open circles) mice. (*b*) Incidence of type I diabetes in male mice. Symbols are the same as in *a*. (*c*) Severity of insulitis in female NOD-*Pdcd1*$^{-/-}$, NOD-*Pdcd1*$^{+/-}$, and NOD WT mice was evaluated at 4 and 6 weeks of age. Insulitis was scored as follows: presence of periinsulitis (grade 1), moderate insulitis (grade 2), and severe insulitis (grade 3), and the percentage of islets with each grade of insulitis was calculated. Black, red, and pink bars represent the percentages of islets with grade 3, grade 2, and grade 1 insulitis, respectively. White bars represent the percentage of islets without inflammation. The data are the mean of at least five mice for each genotype. On average, 203 islets were analyzed from 12 independent sections for each mouse. (*d*) Severity of insulitis in female NOD-*Pdcd1*$^{-/-}$, NOD-*Pdcd1*$^{+/-}$, and NOD WT mice at 6 weeks. Insulitis was scored as in *c*, and the mean score of individual mice is plotted. Bars represent mean value. Symbols are the same as in *a*. (*e*) Hematoxylin/eosin staining of representative islets, parotid glands, and submandibular glands of NOD WT (*Upper*) and NOD-*Pdcd*$^{-/-}$ (*Lower*) mice at 6 weeks.

ing to the published criteria (15). Briefly, grade 1 represents the presence of one to five foci of mononuclear cells (>20 cells per focus), grade 2 represents the presence of more than five foci of mononuclear cells but without significant parenchymal destruction, grade 3 represents the presence of multiple confluent foci with moderate parenchymal degeneration, and grade 4 represents the presence of extensive infiltration with extensive parenchymal destruction. More than four mice were evaluated for each genotype at 6 weeks of age.

Reagents. APC-conjugated streptoavidin, APC-conjugated antibodies against CD3 and B220, Cy5-conjugated antibodies against CD8 and B220, phycoerythrin-conjugated antibodies against CD4 and B220, and FITC-conjugated antibodies against CD8, CD25, CD3, and IFN-γ were purchased from eBioscience (San Diego). Biotinylated antibody against CD11c was purchased from Pharmingen. Polyclonal antibodies against PD-L1 and PD-L2 were purchased from R & D Systems. FITC- and Cy5-conjugated polyclonal antibodies against goat IgG and Texas red-conjugated polyclonal antibody against mouse IgM were purchased from Jackson ImmunoResearch.

ELISA. Serum Ig levels were measured as described in ref. 16. Serum autoantibody against insulin was measured as described in ref. 17.

Immunohistochemistry. Pancreata were collected from indicated animals and snap-frozen in OCT compound. Cryosections were fixed with CytoFix (Pharmingen) and stained with indicated antibodies. Signals were observed with AXIOVISION (Bio-Rad).

Cytoplasmic Staining. Islet-infiltrating cells were collected according to the methods described in ref. 18. Islet infiltrates, splenocytes, or pancreatic lymph node cells were stimulated with 10 ng/ml phorbol 12-myristate 13-acetate and 1 μg/ml ionomycin for 5 h with Goldi-stop (Pharmingen) and stained with antibodies against CD3, IFN-γ, and IL-4. Data were analyzed with a FACSCalibur cell sorter (Becton Dickinson).

Genetic Linkage Analysis. Progenies were monitored for the incidence of diabetes every week by using Uropiece S (Fujisawa Pharmaceutical, Osaka) until 24 weeks of age. Mice were killed 2–4 weeks after the onset of diabetes or at 24 weeks of age and examined for the presence of insulitis. Microsatellite markers used in the first screening are as follows: D1mit65, D1mit18, D1mit8, D1mit150, D1mit155, D2mit429, D2mit433, D2mit37, D2mit338, D2mit26, D2mit265, D3mit227, D3mit106, D3mit128, D4mit1, D4mit178, D4mit31, D4mit187, D5mit294, D5mit81, D5mit188, D5mit191, D6mit184, D6mit263, D6mit256, D6mit373, D7mit191, D7mit82, D7mit105, D7mit242, D8mit287, D8mit65, D8mit211, D8mit156, D9mit91, D9mit208, D9mit346, D9mit321, D10mit124, D10mit259, D10mit12, D10mit180, D11mit21, D11mit87, D11mit41, D11mit181, D12mit171, D12mit214, D12mit133, D13mit61, D13mit9, D13mit78, D14mit50, D14mit129, D14mit225, D14mit177, D15mit139, D15mit121, D15mit159, D16mit131, D16mit11, D16mit106, D17mit113, D17mit68, D17mit93, D18mit94, D18mit186, D19mit23, D19mit19, D19mit66, D19mit71, DXmit119, DXmit117, and DXmit240. Genetic linkage was evaluated by using MAPMANAGER QTX.

Results

Acceleration of Type I Diabetes by PD-1 Deficiency. NOD-*Pdcd1*$^{-/-}$ mice were generated by backcrossing C57BL/6-*Pdcd1*$^{-/-}$ mice on NOD mice for more than five generations and were monitored for the incidence of diabetes. As shown in Fig. 1*a*, some of the female NOD-*Pdcd1*$^{-/-}$ mice became diabetic from 5 weeks of age, and the penetration of the disease reached 100% by 10 weeks. The diabetic phenotypes of the female PD-1 heterozygotes on NOD mice were milder, starting from 13 weeks of age and reaching 60% penetration by 24 weeks of age. By contrast, female NOD WT littermates started to become diabetic from 17 weeks of age, and only 30% of them developed diabetes by 24 weeks of age. The acceleration of NOD diabetes by PD-1 deficiency is more evident in male animals (Fig. 1*b*). None of male NOD mice developed diabetes by 24 weeks of age, whereas male NOD-*Pdcd1*$^{-/-}$ mice began to develop diabetes from 5 weeks of age, and all of them became sick by 11 weeks. Again, the PD-1 heterozygotes showed milder but significant acceleration of diabetic incidence. Male NOD-*Pdcd1*$^{+/-}$ mice started to

become diabetic from 13 weeks of age, and 40% of them developed diabetes by 24 weeks of age. Thus, the onset and frequency of type I diabetes in NOD mice were highly accelerated by the disruption of the PD-1 gene.

We next examined insulitis in NOD-*Pdcd1*$^{-/-}$ mice. Mild periinsulitis was detectable from 2 weeks of age, and destructive insulitis was already found in 21% of the islets by 4 weeks of age in female NOD-*Pdcd1*$^{-/-}$ mice (Fig. 1*c* and data not shown). At 6 weeks, 82% of the islets were affected with severe insulitis (grades 2 and 3) in female NOD-*Pdcd1*$^{-/-}$ mice, whereas <1% of the islets were affected with severe insulitis in female NOD WT mice (Fig. 1 *c* and *e*). Mean insulitis scores of NOD-*Pdcd1*$^{-/-}$, NOD-*Pdcd1*$^{+/-}$, and NOD WT mice at 6 weeks were 0.4, 0.7, and 2.5, respectively (Fig. 1*d*). The results indicate that more severe insulitis, leading to earlier destruction of beta cells, is responsible for the early onset of diabetes in NOD-*Pdcd1*$^{-/-}$ and NOD-*Pdcd1*$^{+/-}$ mice.

NOD mice also develop sialoadenitis, similar to the human Sjögren's syndrome (19). As shown in Fig. 1*e*, sialoadenitis was also accelerated by PD-1 deficiency. The acceleration was more evident in parotid glands than in submandibular glands (mean sialoadenitis scores of NOD-*Pdcd1*$^{-/-}$, NOD-*Pdcd1*$^{+/-}$, and NOD-*Pdcd1*$^{+/+}$ mice at 6 weeks of age were 1.75, 1.4, and 3.7 for parotid glands, respectively, and 0.3, 0.2, and 1.7 for submandibular glands, respectively). However, there was no inflammatory response in other organs, including kidney and heart, which are attacked in *Pdcd1*$^{-/-}$ mice on C57BL/6 and BALB/c backgrounds, respectively (data not shown). In sum, the autoimmune response is predominantly directed against pancreatic islets and salivary glands in NOD-*Pdcd1*$^{-/-}$ mice.

General Similarity of Immunological Pathophysiology Between NOD WT and NOD-*Pdcd1*$^{-/-}$ Mice. We then examined whether PD-1 deficiency induced production of autoantibodies against the pancreas, as previously shown in dilated cardiomyopathy in BALB/c-*Pdcd1*$^{-/-}$ mice (13). Compared with C57BL/6-*Pdcd1*$^{-/-}$ mice, which have been reported to have higher levels of IgA, IgG2b, and IgG3 (20), serum Ig levels of NOD-*Pdcd1*$^{-/-}$ mice were not different from NOD WT mice at 6 weeks of age (Fig. 6*a*, which is published as supporting information on the PNAS web site). The titer of autoantibodies against insulin was also not different from NOD WT mice (Fig. 6*b*), suggesting that acceleration of diabetes in NOD-*Pdcd1*$^{-/-}$ mice may not be due to the augmented production of autoantibodies. The T/B ratio of the splenocytes was slightly reduced in NOD-*Pdcd1*$^{-/-}$ mice, whereas the T/B ratio of the pancreatic lymph nodes was not affected in NOD-*Pdcd1*$^{-/-}$ mice (Fig. 7 *a* and *b*, which is published as supporting information on the PNAS web site). The CD8/CD4 ratio was slightly reduced in the spleen and pancreatic lymph nodes of NOD-*Pdcd1*$^{-/-}$ mice (Fig. 7 *c* and *d*). The number of CD4$^+$CD25$^+$ regulatory T cells was not different in NOD-*Pdcd1*$^{-/-}$ and NOD WT mice (Fig. 7*e*). Diabetes in NOD-*Pdcd1*$^{-/-}$ mice appears to develop with more or less similar pathophysiology to NOD WT mice but with marked acceleration.

Increased Invasion of CD8$^+$ T Cells in NOD-*Pdcd1*$^{-/-}$ Mice. In addition to the increase in the number of lymphocytes in islets of NOD-*Pdcd1*$^{-/-}$ mice (Fig. 1 *c* and *d*), CD4$^+$ and CD8$^+$ T cells seemed to be more invasive; they were always found deeper inside islets in NOD-*Pdcd1*$^{-/-}$ mice than in NOD WT mice at the same degrees of inflammation stage (Fig. 2*a*). Although insulitis started from the boundary of islets and formed a crescent as reported for NOD WT mice, more abundant CD4$^+$ and CD8$^+$ T cells were found inside islets from earlier stages in NOD-*Pdcd1*$^{-/-}$ mice. In contrast, few CD4$^+$ and CD8$^+$ T cells were found inside islets, even in islets with destructive insulitis in NOD WT mice (Fig. 2*a*, grade 3). From the FACS analysis on islet

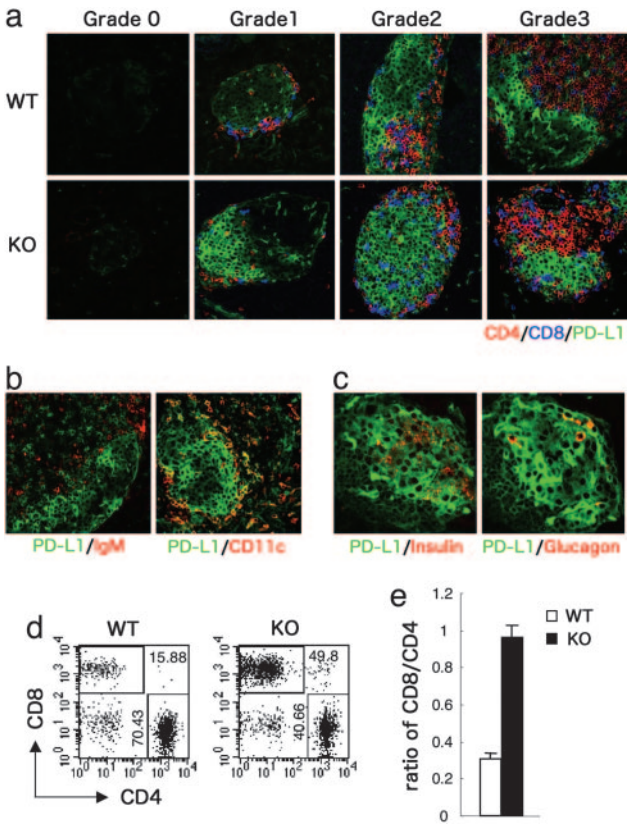

Fig. 2. Invasion of CD8$^+$ T cells in islets and expression of PD-L1 on beta cells. (*a*) CD4$^+$ (red) and CD8$^+$ (blue) T cells and PD-L1$^+$ (green) cells were detected in the islets of grade 0, 1, 2, and 3 insulitis of NOD WT (*Upper*) and NOD-*Pdcd1*$^{-/-}$ (*Lower*) mice. (*b*) PD-L1 expression on B cells (*Left*) and CD11c$^+$ DCs (*Right*) in prediabetic NOD WT mice. Red signal represents IgM$^+$ B cells (*Left*) and CD11c$^+$ DCs (*Right*). Green signal represents PD-L1$^+$ cells. (*c*) PD-L1 is expressed on beta cells (*Left*) and glucagon-producing alpha cells (*Right*) in prediabetic NOD WT mice. Red signal represents insulin$^+$ beta cells (*Left*) and glucagon$^+$ alpha cells (*Right*). Green signal represents PD-L1$^+$ cells. (*d* and *e*) CD8/CD4 ratio of islet infiltrates. (*d*) Representative FACS profiles of islet infiltrates are shown for prediabetic NOD WT and NOD-*Pdcd1*$^{-/-}$ mice. (*e*) Mean CD8/CD4 ratios are shown. Error bars represent standard error.

infiltrates of 6-week prediabetic NOD-*Pdcd1*$^{-/-}$ mice, the CD8/CD4 ratio was increased nearly 3-fold, compared with the disease-matched control of 15-week prediabetic NOD WT mice (Fig. 2 *d* and *e*).

It was reported that PD-L1, but not PD-L2, was up-regulated on islets upon insulitis in NOD WT mice by immunohistochemistry (21, 22). Because the cell types that express PD-L1 were not determined in the previous reports, we performed immunohistofluorescence by using polyclonal antibodies against PD-L1 and PD-L2. PD-L1 was expressed strongly on beta cells as well as CD11c$^+$ dendritic cells (DCs) and moderately on alpha cells, whereas T cells and B cells did not express PD-L1 (Fig. 2 *a–c*). Interestingly, the expression of PD-L1 on beta cells was stronger at the boundary with T cells than inside of islets in NOD WT mice, suggesting that beta cells may suppress activities of PD-1-expressing T cells at the boundary to prevent the invasion of T cells into islets (Fig. 2*a*). Actually, the expression of PD-1 was detected on a small fraction of infiltrating CD4$^+$ and CD8$^+$ T cells of NOD WT mice and up-regulated by *in vivo* blockade of PD-L1 using anti-PD-L1 antibody, suggesting that the expression of PD-1 is not stable in the presence of a continuous interaction with its ligand (data not shown). The expression of PD-L1 was detected more highly and diffusely on islets in NOD-*Pdcd1*$^{-/-}$

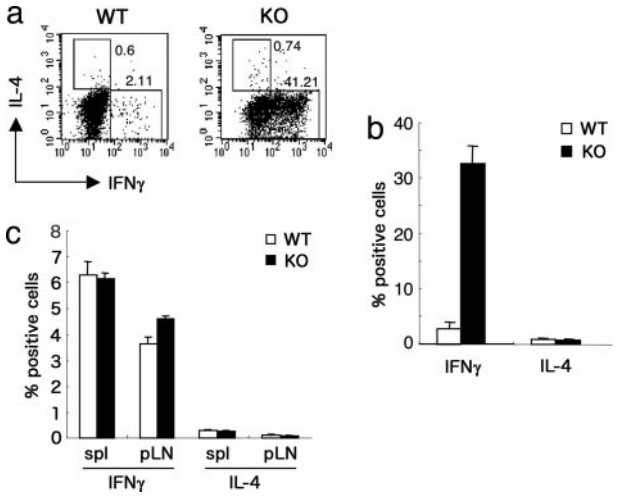

Fig. 3. Th1 response is augmented in the islets of NOD-*Pdcd1*$^{-/-}$ mice. (*a* and *b*) Islet-infiltrating T cells were collected and examined for the production of IFN-γ and IL-4. (*a*) Representative FACS profiles of NOD WT (*Left*) and NOD-*Pdcd1*$^{-/-}$ (*Right*) mice are shown. (*b*) Mean percentage of IFN-γ-producing cells (*Left*) and IL-4-producing cells (*Right*) are shown. White bars represent NOD WT mice and black bars represent NOD-*Pdcd1*$^{-/-}$ mice. Error bars represent standard error. (*c*) Production of IFN-γ (*Left*) and IL-4 (*Right*) by splenocytes (spl) and pancreatic lymph node cells (pLN) was examined as above. Error bars represent standard error.

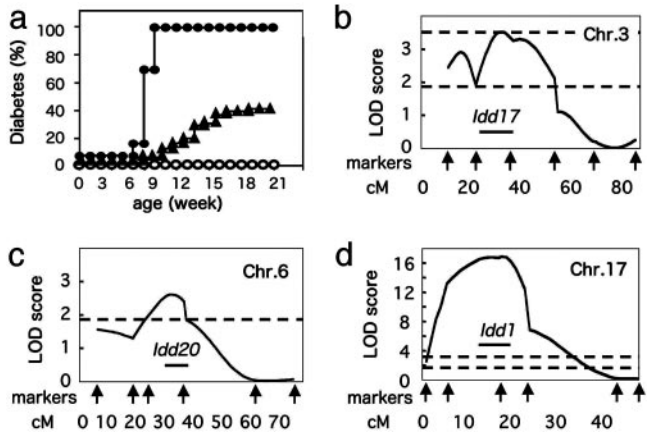

Fig. 4. Genetic association of *Idd1*, *Idd17*, and *Idd20* with diabetic incidence of NOD-*Pdcd1*$^{-/-}$ mice. (*a*) Diabetic incidence of BC1 backcross progenies (NOD-*Pdcd1*$^{-/-}$ × C57BL/6-*Pdcd1*$^{-/-}$)F1 × NOD-*Pdcd1*$^{-/-}$. Filled circles, open circles, and triangles represent cumulative diabetic incidence of NOD-*Pdcd1*$^{-/-}$ and C57BL/6-*Pdcd1*$^{-/-}$ mice and their BC1 progenies, respectively. (*b–d*) Logarithm of odds (lod) score plots for individual chromosomes containing the putative locus controlling diabetic incidence in BC1 progenies. The length of each chromosome is adjusted to the same size, although the centimorgan length of each chromosome varies. Genetic maps were constructed by using MAPMANAGER QTX. Arrows indicate the positions of microsatellite markers used for genotyping. The lod score is given on the *y* axis. Dashed lines indicate the suggestive lod score of 1.9 and the significant lod score of 3.3 (31).

mice, which is probably due to more severe insulitis in NOD-*Pdcd1*$^{-/-}$ mice. Similar to NOD WT mice, PD-L1 was expressed on beta cells, CD11c^{+} DCs, and alpha cells but not on T cells and B cells in NOD-*Pdcd1*$^{-/-}$ mice (data not shown). The expression of PD-L2 was not detected in islets of NOD-*Pdcd1*$^{-/-}$ mice, consistent with the reports on NOD WT mice (refs. 21 and 22 and data not shown).

Islet T Cell Infiltrates Are Strongly Polarized Toward T Helper (Th) 1. Accumulating evidence indicates that Th1 cytokines exacerbate diabetes, whereas Th2 cytokines protect the development of diabetes in NOD mice (23). Thus, we analyzed the Th1/Th2 balance of islet infiltrates in NOD-*Pdcd1*$^{-/-}$ mice. Infiltrating T cells from disease stage-matched prediabetic pancreata of NOD WT (12–15 weeks) and NOD-*Pdcd1*$^{-/-}$ (5–7 weeks) mice were isolated and stimulated *in vitro* for 5 h with phorbol 12-myristate 13-acetate/ionomycin to enhance the cytokine production. The numbers of recovered cells were not different between prediabetic NOD-*Pdcd1*$^{-/-}$ and NOD WT mice in accordance with the matched stages of the insulitis in these mice. As shown in Fig. 3 *a* and *b*, a far larger fraction of T cells from NOD-*Pdcd1*$^{-/-}$ islets produced IFN-γ than those from NOD WT islets. The percentage of IL-4-producing cells was not changed in NOD-*Pdcd1*$^{-/-}$ islets, compared with NOD WT islets. These results indicate that Th1 response is enhanced in the NOD pancreas in the absence of PD-1. Because the increase of IFN-γ-producing cells was not observed in spleen and pancreatic lymph nodes (Fig. 3*c*), the Th1 polarization seems to occur specifically on diabetogenic T cells in islets in NOD-*Pdcd1*$^{-/-}$ mice, which should have been suppressed by the interaction of PD-1 on diabetogenic T cells with PD-L1 on beta cells and/or tissue-resident antigen-presenting cells in NOD WT mice (Fig. 2 *a–c*).

Only 3 of 28 *Idd* Loci Showed Association with Diabetic Incidence by Linkage Analyses Using NOD-*Pdcd1*$^{-/-}$ Mice. Because NOD-*Pdcd1*$^{-/-}$ mice have better features for the type I diabetes model than NOD mice (quick onset and complete penetration), we made intercrosses of NOD-*Pdcd1*$^{-/-}$ mice and C57BL/6-*Pdcd1*$^{-/-}$ mice and performed linkage analysis. We made 201 BC1 progenies by backcrossing (NOD-*Pdcd1*$^{-/-}$ × C57BL/6-*Pdcd1*$^{-/-}$)F1 mice on NOD-*Pdcd1*$^{-/-}$ mice and monitored for the incidence of diabetes for 24 weeks. Seventy-four microsatellite markers were used for the first screening (mean interval = 18.3 cM). As shown in Fig. 4*a*, ≈40% of BC1 progenies developed diabetes by 15 weeks of age. Genetic linkage analyses on BC1 progenies revealed that development of type I diabetes was strongly associated with the D17mit31 and D3mit244 polymorphic markers and weakly associated with the D6mit263 polymorphic marker, which reside in close proximity with *Idd1*, *Idd17*, and *Idd20*, respectively (Fig. 4 *b–d*). By contrast, all of the other known *Idd* loci showed no association with the development of type I diabetes in NOD-*Pdcd1*$^{-/-}$ mice.

Identification of Previously Unrecognized Dominant Loci by Genome-Wide Screening for Dominant Diabetes-Susceptible Loci. Because F2 intercross progenies of NOD WT mice with either of the strains rarely develop diabetes, dominant diabetes-susceptible loci have not been analyzed throughout the genome (7). Because of the high diabetic incidence in NOD-*Pdcd1*$^{-/-}$ mice, dominant diabetes-susceptible genes were screened by F2 crosses. As shown in Fig. 5*a*, ≈20% of the (NOD-*Pdcd1*$^{-/-}$ × C57BL/6-*Pdcd1*$^{-/-}$) F2 progenies developed diabetes by 15 weeks of age. Genetic linkage analyses for dominant loci on 184 F2 progenies using the same maker sets as BC1 analysis revealed strong association with the D17mit239 and D3mit160 polymorphic markers and weak association with the D3mit244 polymorphic marker (Fig. 5 *b* and *c*). D3mit244 resides in close proximity to *Idd17*. Because diabetic loci associated with D3mit160 and D17mit239 have not been pointed out in previous studies, we named these loci *Iddp1* and *Iddp2*, respectively, for *Idd* under PD-1 deficiency. F2 progenies, which are homozygous for C57BL/6 at *Iddp1* and *Iddp2*, rarely developed diabetes [1 of 44 (2.4%) and 0 of 53 (0%), respectively], whereas F2 progenies, which are heterozygous or homozygous for NOD at either *Iddp1* or *Iddp2*, substantially developed diabetes (29.4% and 21.8%, respectively, for *Iddp1* and 20.1% and 45.5%, respectively, for *Iddp2*). Therefore,

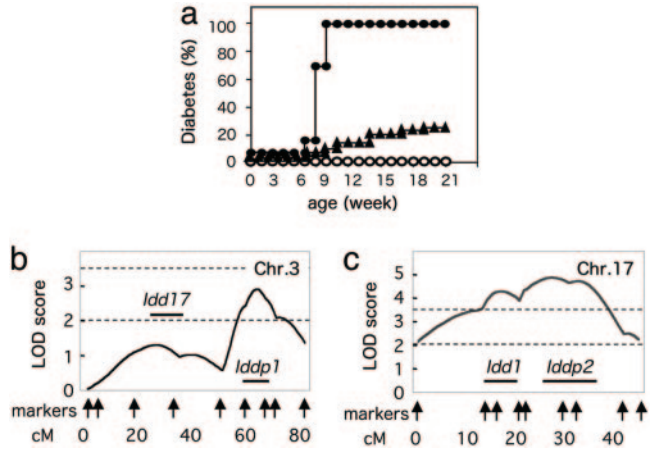

Fig. 5. Identification of *Iddp1* and *Iddp2*. (a) Diabetic incidence of (NOD-*Pdcd1*$^{-/-}$ × C57BL/6-*Pdcd1*$^{-/-}$)F2 progenies. Closed circles, open circles, and triangles represent cumulative diabetic incidence of NOD-*Pdcd1*$^{-/-}$ and C57BL/6-*Pdcd1*$^{-/-}$ mice and their F2 progenies, respectively. (*b* and *c*) lod score plots for individual chromosomes containing the putative dominant locus controlling diabetic incidence among F2 progenies. Dashed lines indicate the suggestive lod score of 2.0 and the significant lod score of 3.4 (31). Representation of chromosomes, lod score, and genetic markers are as described in the legend of Fig. 4.

Iddp1 and *Iddp2* appear to be essential for the development of diabetes.

Discussion

Here, we report that NOD-*Pdcd1*$^{-/-}$ mice develop type I diabetes by 11 weeks of age, with 100% penetration and marked Th1 polarization of islet infiltrates. Augmentation of Th1, but not Th2, response in NOD-*Pdcd1*$^{-/-}$ mice is consistent with the observation on PD-L1-deficient (*Pdcd1lg1*$^{-/-}$) mice. Latchman *et al.* (24) reported that DCs from *Pdcd1lg1*$^{-/-}$ mice induced the augmented production of IFN-γ but not IL-4 in an allogenic mixed lymphocyte reaction compared with DCs from WT mice (24). Several other genetic manipulations on NOD mice have been shown to boost occurrence of diabetes to nearly 100%, including B7.1/B7.2 double knockout and islet antigen-specific T cell receptor (TCR) transgenesis (25–27). In the case of B7.1/B7.2 double-knockout mice, Salomon *et al.* (26) attributed the acceleration of diabetes to the impaired production and activity of regulatory T cells. However, these mice seem to have a wide range of defects in the immune system, as evidenced by the reduced production of both Th1 and Th2 cytokines by T cells and the reduced titer of serum autoantibodies against GAD65, an islet antigen. The islet antigen-specific TCR transgenic mice are destined to be partially immunodeficient, because their CD8$^+$ T cells have a single specificity. Compared with these mice, the immune system of NOD-*Pdcd1*$^{-/-}$ mice are not deviated as we have discussed above; therefore, NOD-*Pdcd1*$^{-/-}$ mice may serve as a useful animal model to analyze the cellular and genetic pathology of type I diabetes.

The requirement of *Idd1*, *Idd17*, and *Idd20* loci for the diabetic incidence of NOD-*Pdcd1*$^{-/-}$ mice suggests that diabetic incidence in NOD WT and NOD-*Pdcd1*$^{-/-}$ mice is regulated by similar polymorphic genes, at least in part. However, the other *Idd* loci did not show association with diabetic phenotypes in NOD-*Pdcd1*$^{-/-}$ mice. Many of the *Idd* loci are supposed to regulate any of the following immune responses: differentiation and expansion of the autoreactive lymphocytes, migration of these autoreactive cells into the pancreas, *in situ* activation of these cells, and destruction of beta cells. Previously, we have reported that PD-1 deficiency augments general immune responses by facilitating the beta selection of T cells in thymus (28), augmenting the activation and proliferation of T and B cells (11, 20) and enhancing the cytotoxic activity of CD8$^+$ T cells (29, 30). PD-1 deficiency may thus overcome the absence of some of the *Idd* loci, which contribute to the diabetic incidence by enhancing general immune responses. If this is the case, it is reasonable that some of the *Idd* loci associated with the general immune regulation did not show any positive association in the current linkage analyses on PD-1-deficient mice. However, *Idd* loci that showed positive association in the current study may be involved in determination of organ specificity toward beta cells in pancreatic islets.

Strong acceleration of diabetes by PD-1 deficiency enabled us to identify previously unrecognized diabetes-susceptible loci (designated *Iddp1* and *Iddp2*), which functioned in a dominant fashion. According to the criteria of statistical significance proposed by Lander and Kruglyak (31), dominant loci analyzed with F2 progenies should have lod scores of >2.0 for suggestive linkage and 3.4 for significant linkage (31). Although *Iddp1* showed only suggestive linkage in the current analysis on 184 F2 progenies, lack of diabetic incidence among F2 progenies homozygous for C57BL/6 at *Iddp1* (1 of 44) implies the high necessity of this locus for diabetic incidence. Because the diabetic incidences of F2 progenies heterozygous or homozygous for NOD at *Iddp1* (29.4% and 21.8%, respectively) are only slightly higher than those of total F2 progenies (20.7%), the sufficiency of this locus for diabetic incidence seems to be not so high, which may be a reason for the low lod value for this locus. Hence, *Iddp1* seems to have a unique property with its essential but not sufficient role in the diabetic incidence of NOD-*Pdcd1*$^{-/-}$ mice. The neighboring region of *Iddp1* contains several genes involved in immune responses, such as caspase 6, small inducible cytokine subfamily E member 1 (*scye1*), NF-κB1, p50, complement component factor i (*cfi*), B cell leukemia/lymphoma 10 (Bcl10), and prostaglandin F receptor. This region has also been reported to have a linkage with susceptibility to experimental allergic encephalomyelitis (*eae10*) and resistance to systemic lupus erythematosus (*Sles3*) using SJL/J and NZW mice, respectively (32, 33).

Iddp2 showed a significant association with the diabetic incidence of NOD-Pdcd1$^{-/-}$ mice. F2 progenies homozygous for C57BL/6 at *Iddp2* were protected from diabetes completely (0 of 53), which assures the high necessity of this locus for diabetic incidence. Compared with *Iddp1*, *Iddp2* showed the dosage effect on the diabetic incidence (0, 20.1, and 45.5% for B6/B6, B6/NOD, and NOD/NOD, respectively), suggesting moderate sufficiency of *Iddp2* on the diabetic incidence of NOD-*Pdcd1*$^{-/-}$ mice. The comparable region of *Iddp2* on the human chromosome locates on the short arm of chromosome 19, which contains a type I diabetes-susceptible locus found in sibling pair families from the United Kingdom (19p13) (34). Although the linkage in the human study is not so strong (maximum lod score = 1.7), there might be a responsible gene common in human and mouse. The candidate genes for the *Iddp2* locus include IL-27, vav1, complement component 3, SH3 domain GRB2-like 1 (*sh3gl1*), regulatory factor times 2 (*rfx2*), TNF ligand superfamily members 7, 9, and 14 (CD70, 4-1BB ligand, and LIGHT, respectively), and thyroid hormone receptor interactor 10 (*trip10*). Although database searches revealed the existence of some missense mutations and deletions in some of the listed genes of NOD mice, currently it is not clear which of the candidate genes are responsible for these loci. Generation of congenic mice for these regions may allow us to identify responsible gene(s) in these loci. These congenic mice may also give us an answer to whether these loci are involved in the diabetic incidence of original NOD mice or just modify the autoimmune response in the absence of PD-1.

Serreze *et al.* (35) analyzed the (NOD × NOR)F2 progenies and found *Idd13*, which functioned in a dominant fashion. However, only 11.6% of the whole mouse chromosome could have been analyzed in their study, because the NOR genome shares ≈88.4% identity with the NOD genome. McAleer *et al.* (36) analyzed the (NOD × NON.H2^{g7})F2 progenies and found *Idd14* and *Idd15*, which also functioned in a dominant fashion. Because NON mice have been segregated from the same colony as NOD mice as a nondiabetic line, their linkage analysis also could not have covered the whole mouse genome. According to their reports, regions around *Iddp1* and *Iddp2* are derived from NOD mice in NOR mice, and the region around *Iddp2* is derived from NOD mice in NON.H2^{g7} mice. Therefore, they could not have identified *Iddp1* and *Iddp2* as dominant loci in their analyses. In the current study, *Idd13*, *Idd14*, and *Idd15* did not show positive association. It is probable that the strong enhancement of immune response by PD-1 deficiency overcomes the absence of these *Idd* loci, as we have discussed for recessive loci. The usage of different strains for control may also explain the negative association of *Idd14* and *Idd15*.

Ansari *et al.* (21) reported that the injection of antibodies against PD-1 or PD-L1, but not PD-L2, into NOD mice accelerated the insulitis and subsequent development of diabetes, suggesting the negative regulatory role of PD-1/PD-L1 in the diabetic incidence of the NOD mouse. Consistent with this report, current findings clearly demonstrated that the PD-1 deficiency accelerates insulitis and subsequent diabetes in the NOD mouse. However, Subudhi *et al.* (37) found costimulatory function of PD-L1 in the autoimmune response against islet antigens by generating PD-L1 transgenic mice under the rat insulin promoter, which spontaneously developed insulitis and subsequently diabetes. One possible explanation for this discrepancy may be a dominant-negative effect of transgenic PD-L1, which may bind but not transduce signal for some unknown reason.

We thank Drs. N. Minato, K. Ikuta, S. Fagarasan, Y. Tanaka, I. Okazaki, and F. Jiang for helpful discussions. This work was supported in part by grants from the Ministry of Education, Science, Sports, Culture, and Technology of Japan.

1. Griffiths, M. M., Encinas, J. A., Remmers, E. F., Kuchroo, V. K. & Wilder, R. L. (1999) *Curr. Opin. Immunol.* **11,** 689–700.
2. Morahan, G. & Morel, L. (2002) *Curr. Opin. Immunol.* **14,** 803–811.
3. Wakeland, E. K., Wandstrat, A. E., Liu, K. & Morel, L. (1999) *Curr. Opin. Immunol.* **11,** 701–707.
4. Delovitch, T. L. & Singh, B. (1997) *Immunity* **7,** 727–738.
5. Yang, Y. & Santamaria, P. (2003) *Diabetologia* **46,** 1447–1464.
6. Deruytter, N., Boulard, O. & Garchon, H. J. (2004) *Diabetes* **53,** 3323–3327.
7. Todd, J. A., Aitman, T. J., Cornall, R. J., Ghosh, S., Hall, J. R. S., Hearne, C. M., Knight, A. M., Love, J. M., McAleer, M. A., Prins, J. B., *et al.* (1991) *Nature* **351**, 542–547.
8. Okazaki, T., Maeda, A., Nishimura, H., Kurosaki, T. & Honjo, T. (2001) *Proc. Natl. Acad. Sci. USA* **98,** 13866–13871.
9. Carreno, B. M. & Collins, M. (2002) *Annu. Rev. Immunol.* **20,** 29–53.
10. Okazaki, T., Iwai, Y. & Honjo, T. (2002) *Curr. Opin. Immunol.* **14,** 779–782.
11. Nishimura, H., Nose, M., Hiai, H., Minato, N. & Honjo, T. (1999) *Immunity* **11,** 141–151.
12. Nishimura, H., Okazaki, T., Tanaka, Y., Nakatani, K., Hara, M., Matsumori, A., Sasayama, S., Mizoguchi, A., Hiai, H., Minato, N. & Honjo, T. (2001) *Science* **291,** 319–322.
13. Okazaki, T., Tanaka, Y., Nishio, R., Mitsuiye, T., Mizoguchi, A., Wang, J., Ishida, M., Hiai, H., Matsumori, A., Minato, N. & Honjo, T. (2003) *Nat. Med.* **9,** 1477–1483.
14. Green, E. A., Eynon, E. E. & Flavell, R. A. (1998) *Immunity* **9,** 733–743.
15. Shim, G. J., Warner, M., Kim, H. J., Andersson, S., Liu, L., Ekman, J., Imamov, O., Jones, M. E., Simpson, E. R. & Gustafsson, J. A. (2004) *Proc. Natl. Acad. Sci. USA* **101,** 12628–12633.
16. Tanigaki, K., Han, H., Yamamoto, N., Tashiro, K., Ikegawa, M., Kuroda, K., Suzuki, A., Nakano, T. & Honjo, T. (2002) *Nat. Immunol.* **3,** 443–450.
17. Kendall, P. L., Woodward, E. J., Hulbert, C. & Thomas, J. W. (2004) *Eur. J. Immunol.* **34,** 2387–2395.
18. Gregory, S., Giarratana, N., Smiroldo, S. & Adorini, L. (2003) *J. Immunol.* **171,** 4040–4047.
19. van Blokland, S. C. & Versnel, M. A. (2002) *Clin. Immunol.* **103,** 111–124.
20. Nishimura, H., Minato, N., Nakano, T. & Honjo, T. (1998) *Int. Immunol.* **10,** 1563–1572.
21. Ansari, M. J., Salama, A. D., Chitnis, T., Smith, R. N., Yagita, H., Akiba, H., Yamazaki, T., Azuma, M., Iwai, H., Khoury, S.J., *et al.* (2003) *J. Exp. Med.* **198,** 63–69.
22. Liang, S. C., Latchman, Y. E., Buhlmann, J. E., Tomczak, M. F., Horwitz, B. H., Freeman, G. J. & Sharpe, A. H. (2003) *Eur. J. Immunol.* **33,** 2706–2716.
23. Rothe, H., Ito, Y. & Kolb, H. (2001) *J. Mol. Med.* **79,** 190–197.
24. Latchman, Y. E., Liang, S. C., Wu, Y., Chernova, T., Sobel, R. A., Klemm, M., Kuchroo, V. K., Freeman, G. J. & Sharpe, A. H. (2004) *Proc. Natl. Acad. Sci. USA* **101,** 10691–10696.
25. Verdaguer, J., Yoon, J. W., Anderson, B., Averill, N., Utsugi, T., Park, B. J. & Santamaria, P. (1996) *J. Immunol.* **157,** 4726–4735.
26. Salomon, B., Lenschow, D. J., Rhee, L., Ashourian, N., Singh, B., Sharpe, A. & Bluestone, J. A. (2000) *Immunity* **12,** 431–440.
27. Adorini, L., Gregori, S. & Harrison, L. C. (2002) *Trends Mol. Med.* **8,** 31–38.
28. Nishimura, H., Honjo, T. & Minato, N. (2000) *J. Exp. Med.* **191,** 891–898.
29. Iwai, Y., Ishida, M., Tanaka, Y., Okazaki, T., Honjo, T. & Minato, N. (2002) *Proc. Natl. Acad. Sci. USA* **99,** 12293–12297.
30. Iwai, Y., Terawaki, S., Ikegawa, M., Okazaki, T. & Honjo, T. (2003) *J. Exp. Med.* **198,** 39–50.
31. Lander, E. & Kruglyak, L. (1995) *Nat. Genet.* **11,** 241–247.
32. Butterfield, R. J., Sudweeks, J. D., Blenkenhorn, E. P., Korngold, R., Marini, J. C., Todd, J. A., Roper, R. J. & Teuscher, C. (1998) *J. Immunol.* **161,** 1860–1867.
33. Nguyen, C., Limaye, N. & Wakeland, E. K. (2002) *Arthritis Res.* **4,** S255–S263.
34. Mein, C. A., Esposito, L., Dunn, M. G., Johnson, G. C., Timms, A. E., Goy, J. V., Smith, A. N., Sebag-Montefiore, L., Merriman, M. E., Wilson, A. J., *et al.* (1998) *Nat. Genet.* **19**, 297–300.
35. Serreze, D. V., Prochazka, M., Reifsnyder, P. C., Bridgett, M. M. & Leiter, E. H. (1994) *J. Exp. Med.* **180,** 1553–1558.
36. McAleer, M. A., Reifsnyder, P., Palmer, S. M., Prochazka, M., Love, J. M., Copeman, J. B., Powell, E. E., Rodrigues, N. R., Prins, J. B., Serreze, D. V., *et al.* (1995) *Diabetes* **44,** 1186–1195.
37. Subudhi, S. K., Zhou, P., Yerian, L. M., Chin, R. K., Lo, J. C., Anders, R. A., Sun, Y., Chen, L., Wang, Y., Alerge, M. L. & Fu, Y. X. (2004) *J. Clin. Invest.* **113,** 694–700.